Dependability-based Reliability Analysis in URC Networks: Availability in the Space Domain

H. V. Kalpanie Mendis, Indika A. M. Balapuwaduge, *Member, IEEE,* Frank Y. Li, *Senior Member, IEEE*

***Abstract*—Ultra-reliable low latency communication (URLLC), which refers to achieving almost 100% reliability at a certain (satisfactory) level of services and stringent latency, is one of the key requirements for 5G networks. However, most prior studies on reliable communication did not address space domain analysis. Neither were they pursued from a dependability perspective. This paper addresses the ultra-reliable communication (URC) aspect of URLLC and aims at advocating the concept of URC from a dependability perspective in the space domain. We perform in-depth analysis on URC considering both the spatial characteristics of cell deployment and user distributions, as well as service requirements. We first introduce the concepts of cell availability and system availability in the space domain, then perform connectivity-based availability analysis by considering a Voronoi tessellation where base stations (BSs) are deployed according to a certain distribution. Moreover, we investigate the relationship between signal-to-interference-plus-noise ratio (SINR), user requirement, and achievable cell or system availability by employing both Poisson point process (PPP) and determinantal point process (DPP) BS distributions. For SINR-based availability analysis, coverage contours are identified. Considering further the user distribution in a region of interest, expressions for system availability are derived from users' perspective. Furthermore, we propose an algorithm which could be used for availability improvement based on the calculated availability level. Numerical results obtained considering diverse network scenarios and cell deployments with multiple cells and multiple topologies illustrate the achievable availability under various circumstances.**

***Index Terms*—URLLC/URC, dependability theory, reliability and availability, space domain analysis, Voronoi tessellation.**

I. Introduction

As an advancement towards a networked society, the fifth generation (5G) network is expected to provide superb services including much higher data rates for enhanced mobile broadband (eMBB), ultra-reliable low latency communication (URLLC), and massive machine type communication (mMTC) connections. In addition, 5G new radio is foreseen to be evolved from long term evolution (LTE) and be highly integrated with wireless fidelity (WiFi) in order to expand the coverage at higher data rates and facilitate seamless user experience. As an integral part of the 5G paradigm, URLLC which provides both ultra-reliable communication (URC) and low latency is envisaged as an important technology pillar for providing anywhere and anytime services to end-users with almost 100% reliability [1]. In addition to providing conventional cellular services, URC is expected to support applications such as entertainments, factory automation, transport industry, and electrical power distribution where reliability and low latency requirements are deemed to be of paramount importance. These novel applications require ultra-reliable connectivity with guaranteed availability and reliability for service provisioning. Moreover, as 5G is moving closer to real-life deployment and operation, the concept of dynamic network topology design and planning has emerged [2]. With this concept, a cellular network should have the capability to react quickly and update its network configurations dynamically in order to adopt to traffic variations and to support new services. As such, availability analysis based on cell coverage and service requirements is not only pivotal in the initial network planning phase but also valuable in the operational and service upgrading phase.

A. Reliability/Availability from a Dependability Perspective

Reliability and availability are two primary attributes defined in dependability theory, representing the essential capability that is expected for a computing or communication system. Conventionally, they are interpreted from the time domain [3]. While reliability describes the ability that a system or network functions without failure under stated conditions *for a specified period of time*, availability represents the ability that the system functions properly *at a specified instant or interval of time*.

Achieving reliable communication in mobile and wireless networks is particularly challenging, due to the intrinsic nature of such networks. In the literature, two categories of approaches for providing reliable communications exist, i.e., from the traditional quality of service (QoS) perspective and from the dependability theory perspective. With respect to the metrics used to characterize reliable communication from the QoS perspective, parameters such as packet delivery ratio (PDR), packet reception ratio (PRR), bit error rate (BER) or frame error rate (FER), signal-to-interference-plus-noise ratio (SINR), and outage probability are extensively adopted. These approaches represent the conventional understanding of reliable communication and thus lack perceptions from the dependability perspective.

To provide URLLC/URC services in 5G networks from a dependability perspective, it is essential to analyze the dependability attributes of such a system since dependability metrics describe quantitatively the fundamental properties upon which a system can operate satisfactorily. In the context of the dependability theory, metrics such as mean up time (MUT), mean down time (MDT), mean time to failure (MTTF), and mean

Manuscript received October 18, 2018; revised May 5, 2019 and June 19, 2019; accepted July 26, 2019; approved by IEEE/ACM TRANSACTIONS ON NETWORKING Editor K. Tang. Date of publication XXXXX YY, 2019; date of current version XXXX YY, 2019. *(Corresponding author: F. Y. Li.)*

The authors are with the Department of Information and Communication Technology, University of Agder (UiA), N-4898 Grimstad, Norway (email: kalpaniemendis89@gmail.com; {indika.balapuwaduge; frank.li}@uia.no).

This paper has supplementary downloadable material available at http://ieeexplore.ieee.org, provided by the authors.

Digital Object Identifier

time to repair (MTTR) have been defined to investigate the reliability aspect of a system [4]. However, these dependability terminologies are applicable merely to the time domain, *not to the space domain*. Therefore it is of vital importance to conduct dependability analysis *also* in the space domain since the dependability of a system may vary with location related parameters [5]. Moreover, availability analysis in the space domain facilitates in-depth comprehension on how to enhance reliability from both *anytime* and *anywhere* perspectives.

B. Contributions

Although URLLC or URC is attracting lots of attention recently, there exists a void in *understanding space domain availability* from a dependability perspective. This paper consolidates the concept of space domain availability proposed in our prior work [5] and extends the availability analysis towards SINR-based and user-oriented analysis by considering various topologies as well as BS and user distributions. Such an in-depth analysis could help to find means for achieving URC and for providing services at both anytime and anywhere. Since a network operator needs to upgrade or fine-tune its deployed network to facilitate new services or maintain the agreed QoS level despite traffic volume increase, the analysis framework provided in this paper may help them for decision making both during and after the network planning phase.

The main objective of this work is to advocate and reinforce space domain definitions on cell and system availability from a dependability theory perspective and perform availability analysis in spatially modeled cellular networks. Briefly, the main contributions of this work are highlighted as follows.

1) The concepts of cell and system availability in cellular networks in the space domain are elaborated and reinforced from the perspective of dependability theory.
2) A connectivity-based analysis for cell and system availability is performed considering a Voronoi tessellation network with multiple cells and multiple topologies. The analysis is performed based on both Poisson point process (PPP) and determinantal point process (DPP).
3) The space domain availability analysis is extended by taking SINR as a criterion for achieving required availability. The analysis is performed by obtaining the coverage contours which define the boundary of exceeding the minimum achieved SINR thus the required availability.
4) Considering that the user equipment (UE) distribution also follows a homogeneous two-dimensional PPP, the concepts of both individual user availability and user-oriented system availability are introduced and analyzed in the space domain.
5) An algorithm that can be adopted by operators to take actions based on the observed availability level has been proposed and an example of such an action is given.

The rest of this paper is organized as follows. In Sec. II, the related work is summarized and then we present some preliminaries and system overview in Sec. III. Thereafter the advocated space domain availability definitions are elaborated in Sec. IV. The connectivity-based space domain cell and system availability analysis is performed in Sec. V, followed by SINR-based analysis in Sec. VI. Then the user-oriented analysis is performed in Sec. VII. In Sec. VIII, we explain the algorithms for availability calculations. Furthermore, the obtained numerical results are presented in Sec. IX. In Sec. X, we propose an algorithm for cell availability improvement and finally the paper is concluded in Sec. XI.

II. Related Work

URC is a novel topic which emerged along with 5G networks. So far the research work in this field is still in its initial phase. In what follows, we briefly summarize the related work to this topic from four different angles, i.e., URC terminology and initial efforts; QoS-oriented approaches; dependability-oriented approaches; and stochastic geometry analysis of cellular networks.

A. URLLC/URC terminologies and initial efforts

The concept of URC was initiated by the EU METIS project which had the goal of laying the foundation of 5G [6]. The terminology evolves to URLLC and it is currently under investigation by the 3rd generation partnership project (3GPP) to become part of the 5G standard (3GPP Release 16) [1]. In addition to an insight on the terminology of URC, [7] presented several motivating scenarios for supporting URC in future wireless applications. In [6], it is stated that availability is an assessment area criterion describing the percentage of places inside a coverage area where a service is provided to end-users with the requested quality of experience (QoE) level. Alternatively, it also proclaims that availability is the percentage of users or communication links for which the QoE requirements are fulfilled within a certain geographical area.

B. QoS-oriented approaches

QoS-oriented reliability approaches in the literature have mainly focused on how to provide reliable transmission in communication especially wireless communication networks. For example, [8] defined reliability as the probability of a packet being successfully decoded in a data transmission or through retransmissions. The performance of fiber-wireless (FiWi) enhanced LTE-Advanced (LTE-A) heterogeneous networks was evaluated in [9] by focusing particularly on the 5G key attributes of very low latency and ultra-high reliability. In [10], the relationship between packet loss rate at the physical layer and signal-to-noise ratio (SNR) in IEEE 802.15.4 networks was investigated. Furthermore, a derivation for a reliability metric, PDR, was presented in [11] considering homogeneous k-dimensional PPP ad hoc networks.

C. Dependability-oriented approaches

The up-to-date research work performed in this category has traditionally focused on the time domain. Based on dependability theory, several reliability and availability metrics were defined in [12] for channel access in multi-channel cognitive radio networks. [13] introduced availability as a novel metric for URC to estimate the presence or absence of link reliability at the time of transmission. Aiming at facilitating availability analysis *in the space domain*, we initiated the concepts of cell and system availability in our earlier work [5]. Therein, we performed a connectivity-oriented cell-wise and system-wise availability analysis based on stochastic geometry which is a

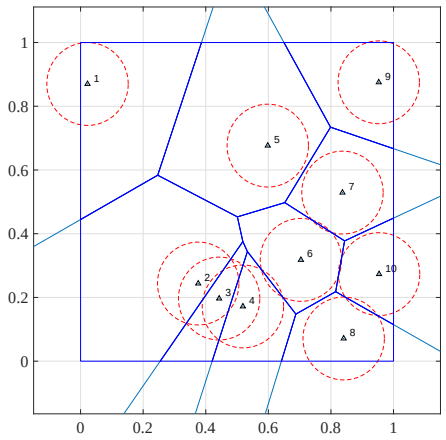

The cell boundaries are shown and the cells together form a Voronoi tessellation. The Voronoi cell boundaries which create the actual geographical area of each cell are indicated in blue (solid) lines. The BS coverage which the BS can communicate with the UE within each cell is indicated in red (dashed) lines.

Fig. 1: Topology 1: A PV distributed homogeneous cellular network consisting of 10 cells, with one BS in each cell.

popular tool to model the randomness incorporated in cellular networks. Moreover, a joint time-space availability analysis which includes QoS in the reliability metric definition was performed in [14].

D. Stochastic geometry for cellular network analysis

Many prior studies including [15][16][17] adopted PPPs to model the distribution of base stations (BSs) in modern cellular networks. In [18], the outage probability for mobile users was analyzed in order to optimize BS deployment density and achieve optimal network performance. [19] used a PPP to model single tier networks and obtained tractable results for SINR, coverage probability, and average rate of users. Furthermore, a model to analyze the coverage probability for PPP based heterogeneous networks was presented in [23]. The probability of a user being connected to a macro cell or open access femto cell was computed in [24] by using realistic stochastic geometry models. Moreover, [25] investigated the coverage probability and the SINR distribution in non-homogeneous PPP networks. Although other BS distributions are also reported [26], PPP is the most tractable and widely used model for the analysis of wireless networks [19][20]. However, PPP returns random network topologies without any limitations on the minimum distance between neighboring transmitters. To overcome this drawback, another type of BS distribution, known as DPP, has also been investigated [21]. The main advantage of DPP modeling is the possibility to represent the repulsiveness among macro BSs, i.e., the fact that BSs are not installed very close to each other. Note however that none of the related work summarized in this subsection is targeted at performing reliability or availability analysis from a dependability perspective.

III. Preliminaries and System Overview

In this section, we first revisit the basic concepts which need to be incorporated in our study and then explain network scenarios. Our observations on coverage holes in a real-life operational cellular network are also presented.

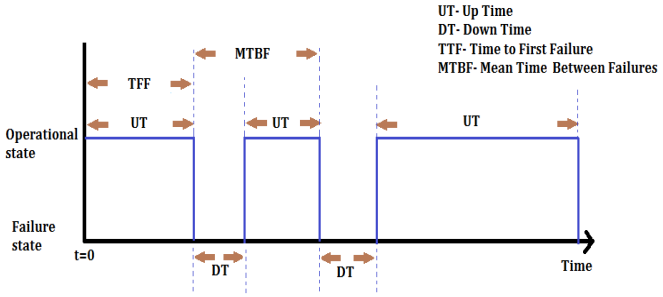

Fig. 2: Illustration of the time domain availability definition.

A. Preliminaries on Reliability and Availability

Reliability, as one of the primary attributes of the dependability theory, has been widely deemed as an important aspect of both wired and wireless networks. In general, a given system may be required to perform specific functions at different reliability levels. According to [27], reliability is defined as *the probability that a system will perform its intended functions without failure for a given interval of time under specified operating conditions*.

In reality, however, only a handful of systems can operate continuously without interruption and failures. In most of the time, we are not only interested in the probability of failure occurrence but also the fraction of time or space in which the system is in the operational mode, represented by availability. For the definition of time domain availability for a repairable system, refer to ITU-T recommendation E.800 [3].

B. Voronoi Tessellation and Network Scenarios

In stochastic geometry, Voronoi tessellation is a popular approach for spatially modeling real-life cellular networks. Given a set of centers or seeds, a Voronoi tessellation can partition a region of interest into multiple polygon areas, known as Voronoi cells. These cells do not overlap with each other and collectively cover the whole region of interest. Each of the cells contains those points inside the region that are closest to the seed of the cell that they are associated with.

Consider a cellular network which is deployed following the Poisson Voronoi (PV) principles. For ease of analysis, we focus on a 1×1 unit region of a cellular network which forms a Voronoi tessellation consisting of N number of cells, as shown in Fig. 1. Furthermore, the N cells considered in this network can be spatially distributed in a multiplicity of topologies. In Fig. 1 and Fig. 3, we illustrate respectively 1 and 4 random topologies of a PPP distributed cellular network with $N = 10$ cells. In the rest of this paper, Topology 1 illustrated in Fig. 1 serves as the reference topology for our *single topology* scenario. Together with this topology, the four other topologies illustrated in Fig. 3 form the *multiple topology* scenario which represents different cell deployments of *the same network*.

C. Observation of Coverage Holes in Real-life Networks

According to [22], a coverage hole is an area where the signal level SNR (or SINR) of both serving and allowed neighbor cells is below the level needed to maintain a basic service. If located in a coverage hole, a user will suffer from service unavailability like call drop or radio link failure.

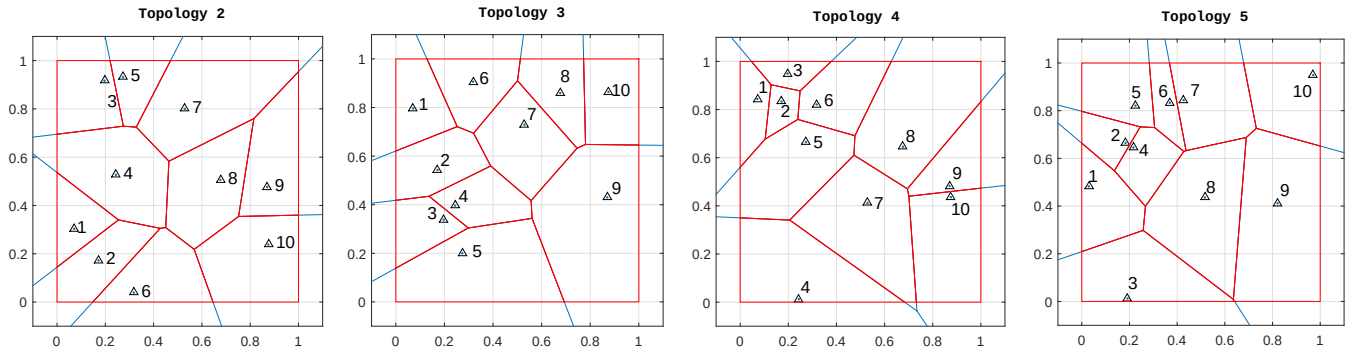

Fig. 3: Four topologies for a PPP distributed cellular network with 10 cells. The BS locations are represented by a triangle in each cell.

To observe possible coverage holes in real-life operational networks, we illustrate in Fig. 4 a zoomed-in picture of the coverage area of 4G+/LTE-A mobile data services provided by Telia, which is the second largest mobile operator in Norway, shown as the coverage in (a) Norway; (b) the Agder region; and (c) a portion of the Grimstad municipality, respectively. As can be observed, coverage holes do exist at certain places. Furthermore, it is worth mentioning that coverage holes are service dependent due to different QoS requirements. Indeed, in the same region as shown in Fig. 4(c), we have observed full coverage for 4G/LTE services but larger coverage holes for LTE-MTC (LTE-M) services.

IV. Space Domain Availability Definitions

In this section, we consolidate the advocated space domain availability definitions. In a nutshell, the availability of a system is the probability that the system is functioning properly under given conditions at the instant (or during a period) of time or the point (or within an area) of space. While the time domain network availability deals with the anytime aspect of URC, the space domain network availability addresses the anywhere aspect of URC.

A. Time Domain Availability Concepts

Before developing our concept which defines network availability in the space domain, let us first revisit the time domain definition of availability. When the system is in a state in which it is able to allocate the requested resource (a communication channel, required SNR, etc.) to a user, the system is said to be in the operational state. Otherwise, the system is said to be in the failure state. Correspondingly, the available time or uptime (UT) is the time during which the system is operational. Otherwise, the system is in the failed state or downtime (DT). We elaborate these terms in Fig. 2. Let MUT and MDT denote the mean value of UT and DT times respectively. Accordingly, for a repairable system, the steady state availability in the time domain, A_t, is defined as,

$$A_t = \frac{MUT}{MUT + MDT}. \tag{1}$$

B. Space Domain Availability Definitions

Analogous to the time domain, we define the space domain availability of a cellular network as follows. The network availability in the space domain is decided as the ratio between the *covered area* by the BS(s) and the *total area* of the cell or network of interest. Note that the covered area can be decided by using different criteria.

Consider the randomness of cell sizes in stochastic geometry cellular networks. Denote the mean covered area and the mean uncovered area as MCA and MUA respectively. The *covered area of a BS* means the geographic area within which a randomly distributed UE is covered (according to a specific criterion) by the BS. On the other hand, the *area of a cell* means the actual geographic area confined by the boundaries of a Voronoi cell. Typically in a cellular network, not all points in the *area of a cell* can be covered by the *covered area of a BS*, as illustrated in Fig. 5.

Analogous to (1), we define the space domain availability, denoted by A_s, as follows,

$$A_s = \frac{MCA}{MCA + MUA}. \tag{2}$$

Accordingly, the space domain unavailability, denoted by U_s, is obtained as follows,

$$U_s = 1 - A_s. \tag{3}$$

The goal of achieving URC in the space domain is to diminish unavailability to a sufficiently low level.

V. Connectivity-based Availability Analysis

In this section, we explore the concept of space domain availability to perform cell availability and system availability analysis. Herein, we adopt connectivity as the criterion for our availability analysis and consider from single cell and single topology to multiple cells and multiple topologies.

A. Cell Availability

Cell availability is the space domain availability defined for a single cell or multiple cells of interest. The cell of interest may be a specific cell in a given topology, e.g., Cell 6 in Fig. 5, or the same cell across multiple topologies. Moreover, we consider also multiple cells in a single topology, or across multiple topologies.

1) Single cell single topology (SCST): Consider a single Voronoi cell, i, which is arbitrarily selected among N randomly deployed cells for a given topology, j, where $j = 1, 2, ..., M$ and M is the total number of topologies deployed.

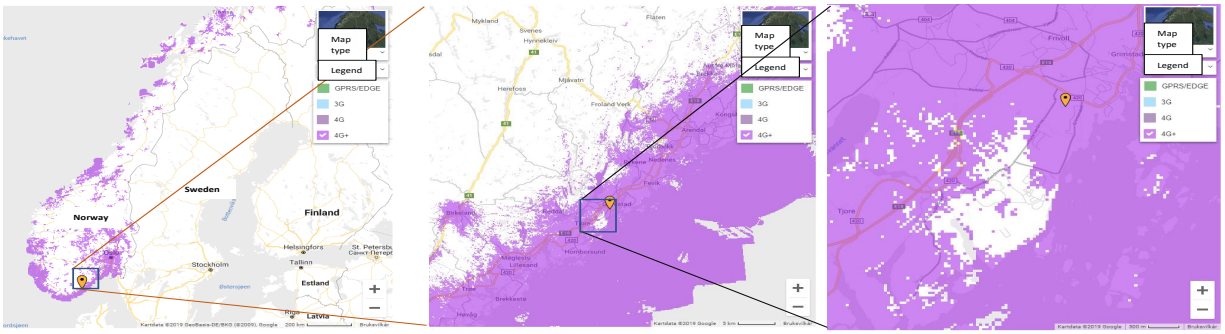

(a) Norway (b) Agder region (c) Grimstad Area

Fig. 4: Coverage illustration of 4G+/LTE-A mobile data services for Telia in Norway: A zoomed-in picture. The purple color represents the areas with 4G+/LTE-A coverage whereas the white spots indicate the uncovered areas, i.e., coverage holes.

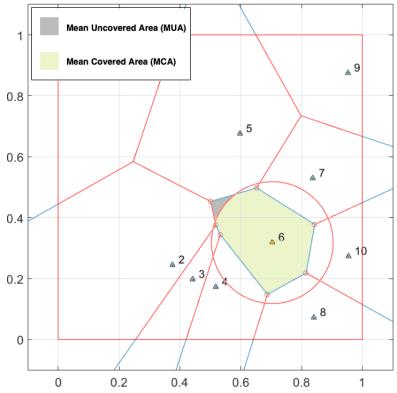

Fig. 5: Illustration of MCA and MUA for Cell 6 in a 10-cell PV network. The red circle illustrates the coverage area of the BS assuming omni-directional antennas at the BSs.

The cell availability of the i^{th} cell in the j^{th} network topology, denoted as $A_s^c(i,j)$, is defined as the covered area of the BS deployed in this cell divided by the the area (or size) of the corresponding Voronoi cell. Denote the covered area of cell i when it is in the j^{th} topology by $C(i,j)$ and the area of the i^{th} Voronoi cell of the j^{th} topology by $S(i,j)$. Then SCST cell availability, $A_s^c(i,j)$, is obtained as follows

$$A_s^c(i,j) = \begin{cases} \frac{C(i,j)}{S(i,j)}, & \text{if } C(i,j) < S(i,j); \\ 1, & \text{otherwise.} \end{cases} \tag{4}$$

Furthermore, the cell unavailability of cell i under network topology j, denoted by $U_s^c(i,j)$ is defined as,

$$U_s^c(i,j) = 1 - A_s^c(i,j). \tag{5}$$

2) Single cell multiple topology (SCMT): Consider M randomly deployed topologies of a Voronoi network, all with the identical number of N cells. We obtain a more general definition of cell availability for a particular cell of interest, i, by defining the SCMT cell availability as the average cell availability of the same cell across M network topologies. Denoting it by $A_s^c(i,:)$, it is expressed as follows

$$A_s^c(i,:) = \frac{1}{M}\sum_{j=1}^{M}\left(\frac{C(i,j)}{S(i,j)}\right). \tag{6}$$

3) Multiple cell single topology (MCST): For a given network topology, say j, we can also obtain the cell availability for the whole network by calculating the cell availability for *each individual cell* in the same network and then taking the average value. Accordingly, the MCST cell availability for a randomly selected network topology j consisting of N cells, denoted by $A_s^c(:,j)$, is expressed as follows

$$A_s^c(:,j) = \frac{1}{N}\sum_{i=1}^{N} A_s^c(i,j). \tag{7}$$

4) Multiple cell multiple topology (MCMT): Consider now all N cells in all M network topologies. We obtain the most generic definition of cell availability under the MCMT case. Denoting it by $\bar{A}_s^c$, it can be calculated by either averaging $A_s^c(:,j)$ over M topologies or $A_s^c(i,:)$ over N cells.

$$\bar{A}_s^c = \frac{1}{M}\sum_{j=1}^{M} A_s^c(:,j) = \frac{1}{N}\sum_{i=1}^{N} A_s^c(i,:), \tag{8}$$

and therefore,

$$\bar{A}_s^c = \frac{1}{N}\sum_{i=1}^{N}\left(\frac{1}{M}\sum_{j=1}^{M} A_s^c(i,j)\right) = \frac{1}{MN}\sum_{i=1}^{N}\sum_{j=1}^{M} A_s^c(i,j). \tag{9}$$

B. System Availability

By system availability, we calculate the average space domain availability of *a network* which consists of N cells. Accordingly, system availability is defined *for the whole network* of interest considering the total coverage area collectively provided all BSs within the same network. Different from cell availability, *the overlapping among BS coverages needs to be excluded* when calculating system availability.

1) Single topology: For a specific network topology, j, the system availability, $A_s^s(j)$, is defined as the ratio between the sum of the total covered area of all individual cells and the total area of the network including all N cells. That is,

$$A_s^s(j) = \begin{cases} \frac{\sum_{i=1}^{N} C(i,j) - \Delta}{\sum_{i=1}^{N} S(i,j)}, \\ \quad \text{if } \sum_{i=1}^{N} C(i,j) - \Delta < \sum_{i=1}^{N} S(i,j); \\ 1, \text{ otherwise} \end{cases} \tag{10}$$

where Δ represents those overlapped coverage areas among neighboring BSs and the 'exurban' areas of outer-tier cells. While an overlapping area is an area mutually covered by two or more neighboring BSs, an exurban area is the area which belongs to an outer-tier cell but falls outside the region of

interest, i.e., beyond the 1×1 border. Moreover, the total area of the network equals to 1 if a 1×1 unit area is considered.

2) Multiple topologies: Considering that multiple topologies may be deployed for the same network, we obtain a more generic expression for system availability. For M randomly deployed topologies of a cellular network each with N cells, its system availability, $\bar{A}_s^s$, is expressed as,

$$\bar{A}_s^s = \frac{1}{M} \sum_{j=1}^{M} A_s^s(j). \tag{11}$$

VI. SINR-based Availability Analysis

Although the space domain availability concept and the availability definitions presented in the above two sections apply generally to any availability analysis in the space domain, the coverage areas in these expressions may vary according to different criteria. In this section, we derive expressions for cell availability and system availability based on the received SINR levels over a distance, i.e., the service is regarded as available only if the received SINR is equal to or higher than a predefined threshold. For this reason, the SINR-based coverage area is no longer circular which is an ideal case assumed in [5].

For the sake of analysis simplicity, we assume that all BSs are deployed with identical transmit power in the Euclidean plane. The distribution of the BSs follows a given distribution, e.g., PPP or DPP, and the cells in the region of interest together form a Voronoi tessellation. At the center of each cell, one BS is placed with an omni-directional antenna and the frequency reuse factor of the network is one. An identical propagation condition is assumed for all cells. Each UE is associated with a serving BS according to a given criterion, e.g., distance or SINR. Other cell association schemes, for instance considering load balancing among neighboring cells, may also apply but to design such a scheme is beyond the scope of this paper.

A. SINR and Coverage

Reliable communication in a cellular network may be achieved when the minimum SINR requirement is met at the receiver. Due to signal propagation attenuation, interference from other users, or other reasons, a UE which is covered by a BS under ideal channel conditions may not be associated with the BS if its received SINR is not high enough.

Consider an orthogonal frequency division multiplexing (OFDM) based cellular cell with a number of OFDM sub-carriers serving multiple users. The $SINR^{p,q}$ for the q^{th} OFDM sub-carrier of user p can be simply expressed as [28] $SINR^{p,q} = S_r^{p,q}/(N_p + I^{p,q})$, where $S_r^{p,q}$ denotes the received signal power and $I^{p,q}$ is the interference for the q^{th} sub-carrier of the p^{th} user and N_p represents the noise level at the p^{th} user.

Assuming that the interference term $I^{p,q}$ in the denominator of the above expression is much stronger than the noise term N_p, our analysis could be simplified by ignoring N_p. Accordingly, $SINR^{p,q}$ can be reformulated by using propagation loss to represent $I^{p,q}$, expressed as

$$SINR^{p,q} = \frac{L_p}{\sum_{\substack{i=1 \\ i \neq p}}^{Z} L_i} \tag{12}$$

where L_i is the propagation loss between the transmitter and the receiver for the i^{th} user and Z is the number of co-channel users including the p^{th} user itself and the other $Z-1$ co-channel interferers.

To obtain L_i terms, various propagation models may be applied. For expression simplicity, we give an expression of L_p based on a free space propagation model as follows

$$L_p = \frac{\lambda^2}{(4\pi)^2 (d_p)^{\alpha}} \tag{13}$$

where d_p is the distance between the p^{th} user and the BS, λ is the wavelength of the transmitted signal, and α is the path loss exponent. By substituting (13) into (12), we obtain a simplified expression which relates SINR for the q^{th} OFDM sub-carrier of the p^{th} user and distance d, shown as follows

$$SINR^{p,q} = \frac{(d_p)^{-\alpha}}{\sum_{\substack{i=1 \\ i \neq p}}^{Z} (d_i)^{-\alpha}}. \tag{14}$$

By pre-configuring an appropriate SINR threshold as the minimum SINR requirement that a UE must meet in order to receive services from the BS, we figure out the maximum allowable distance within which the UE is served by the network. Note that for the SINR calculation presented later, we consider only co-channel interference to a UE from neighboring BSs. If the distance between a UE and the BS is shorter than or equal to this distance, we regard the UE as a user within *the covered area* of the corresponding BS. For SINR-based space domain availability, *the covered area of a BS* will be a *contour*, decided by the SINR threshold.

B. SINR-based Cell Availability

Bringing forward the concept of space domain availability as proposed in (2), we define the SINR-based cell availability as the area confined by the coverage contour which satisfies the required minimum SINR threshold divided by the total area of the cell of interest. Correspondingly, we express the SINR-based cell availability in the space domain, $A_s^c(i,j)$, as

$$A_s^c(i,j) = \begin{cases} \frac{C_{SINR}(i,j)}{S(i,j)}, & \text{if } C_{SINR}(i,j) < S(i,j); \\ 1, & \text{otherwise} \end{cases} \tag{15}$$

where $C_{SINR}(i,j)$ denotes the area covered by the SINR-based coverage contour for a randomly selected cell i of topology j.

To provide coherent definitions as proposed in Sec. V, we have also developed cell availability definitions for SCMT, MCST and MCMT scenarios when adopting SINR as a criterion. However, the respective analytical expressions are not presented here due to the page limit.

C. SINR-based System Availability

Similar to the definition in (10), the SINR-based system availability is meant for the whole network considering the total area *collectively covered by the SINR-based coverage contours of all cells* over the total area of the network. Accordingly, we express the SINR-based system availability for a particular topology j, $A_s^s(j)$, as

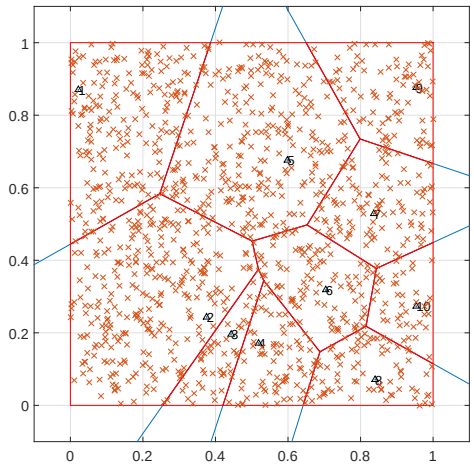

Fig. 6: A PV cellular network in the Euclidean plane with N = 10 BSs distributed according to a homogeneous PPP of intensity $\lambda_B = 10$ and a collection of UEs following another independent homogeneous PPP of intensity $\lambda_U = 1500$.

$$A_s^s(j) = \begin{cases} \frac{\sum_{i=1}^{N} C_{SINR}(i,j) - \Delta}{\sum_{i=1}^{N} S(i,j)}, \\ \quad \text{if } \sum_{i=1}^{N} C_{SINR}(i,j) - \Delta < \sum_{i=1}^{N} S(i,j); \\ 1, \qquad \text{otherwise} \end{cases} \tag{16}$$

where Δ has the same meaning as explained under (10), however, using SINR as the criterion for coverage calculation. Furthermore, the SINR-based system availability for multiple topologies has the same expression as illustrated in (11).

VII. User-oriented Availability Analysis

In this section, we conduct an availability analysis from an end-user's perspective. To perform the analysis, the UE locations are assumed to form a realization of a homogeneous two-dimensional spatial distribution. In what follows, we introduce the concepts of individual user availability and user-oriented system availability in the space domain.

The UEs in the studied network are assumed to be distributed either uniformly (for connectivity-based and SINR-based analysis presented above) or based on another independent homogeneous PPP with intensity λ_U in the Euclidean plane (for user-oriented availability analysis).

A. Network Scenario

Consider a cellular network which consists of N randomly deployed cells each with a BS distributed according to a homogeneous PPP, the same as the one shown in Fig. 1. Additionally, we assume that a number of UEs are distributed randomly in the same network following another independent homogeneous PPP. The intensities for these two PPPs are λ_B and λ_U respectively where $\lambda_U \gg \lambda_B$. Fig. 6 illustrates the network scenario for user-oriented availability analysis.

B. Individual User Availability

Let us first focus on a randomly selected UE located inside the network. If the location of the selected user, m, falls within the covered area of a BS, the *individual user availability in the space domain* for this UE, denoted by $A_s^u(m)$, is 1. Otherwise, $A_s^u(m)$ is 0, since this user cannot be served by any BS. Accordingly, $A_s^u(m)$ becomes binary, as

$$A_s^u(m) = \begin{cases} 1, & \text{if end-user } m \text{ is covered;} \\ 0, & \text{otherwise.} \end{cases} \tag{17}$$

Similar to (3), the individual user unavailability for user m in the space domain, $U_s^u(m)$, is given by $U_s^u(m) = 1 - A_s^u(m)$. Note anyhow that the covered area of a BS can be decided by different criteria.

C. User-oriented System Availability

Now consider the whole population of UEs distributed in this network. We define *user-oriented system availability in the space domain* as follows. This system availability determines the availability of services that BSs provide collectively to UEs which are dispersed within a region of interest.

Consider the same multi-cell scenario as discussed in the previous subsection. The coverage contour of each cell can be obtained by applying a specific criterion, e.g., circular or SINR-based. Let $N_{covered}$ be the total number of users inside the covered areas including all N cells in this network and N_{total} be the user population inside this network. We define user-oriented system availability, A_s^u, as the ratio between $N_{covered}$ and N_{total}, i.e.,

$$A_s^u = \frac{N_{covered}}{N_{total}}. \tag{18}$$

Note that $N_{covered} \leq N_{total}$ since each UE will be associated with at most one BS. Correspondingly, the user-oriented system unavailability, U_s^u, is expressed as $U_s^u = 1 - A_s^u$.

VIII. Procedure and Algorithms for Space Domain Availability Calculations

To calculate the space domain availability defined in the above sections, we need to create Voronoi diagrams, calculate the area of each cell and the covered area of a BS according to different criteria, as presented in the following subsections. A Poisson Voronoi tessellation (PVT) network based procedure is presented in this section as an example to illustrate how to obtain space domain availability according to Algorithm 1. Note however that the space domain availability definitions as well as the cell and system availability expressions presented above are not dependent on a PPP or DPP distribution assumption. That is, they can be applied to other spatial distributions for BSs and UEs as well.

A. Generate a Voronoi Diagram

Given a set of random seeds or centers, a Voronoi diagram in the two-dimensional space can be sketched using the perpendicular bisection method [29]. Starting from a given point C_0, the nearest neighboring seed C_1 can be detected. Then the perpendicular bisector of the line C_0C_1 is created, forming the first edge of the Voronoi polygon corresponding to C_0. Afterwards the second nearest neighboring seed C_2 was

detected, and the perpendicular bisector on C_0C_2 became the second edge of the Voronoi polygon. This algorithm continues with the third (C_3), fourth (C_4), ..., nearest seeds, until the perpendicular bisectors on C_0C_3, C_0C_4, ..., creating a closed polygon which does not change after adding any more distant points. After applying the above procedure for all centers in the considered network, the Voronoi tessellation for the whole network is generated.

B. Size of a Voronoi Polygon: A Deterministic Expression

To deterministically compute the area of each Voronoi polygon in a PVT, the well-known *shoelace formula* is adopted. It is a mathematical algorithm to calculate the area of a simple two-dimensional polygon whose vertices are represented by ordered pairs in the plane [30]. Let (x_l, y_l) be the coordinates of vertex l and v be the number of edges of the Voronoi polygon. Then the formula to calculate the area of the Voronoi polygon, denoted as S, is expressed as,

$$S = \frac{1}{2}\left|\sum_{l=1}^{v-1} x_l y_{l+1} + x_v y_1 - \sum_{l=1}^{v-1} x_{l+1} y_l - x_1 y_v\right|. \quad (19)$$

C. Connectivity-based Availability Calculation

For connectivity-based cell availability analysis, the four combinations of cell and network topologies described in Subsec. IV-A are considered. To evaluate the cell availability for the SCST scenario, first the PV diagrams are generated and then the area of each cell is determined using (19) which gives the value of $S(i,j)$ in (4). For connectivity-based availability calculation, we assume an ideal propagation condition so that the area covered by a BS, i.e., $C(i,j)$, can be simply represented by a circular shape as πR^2 where R is the transmission range of the BS. Then (4) is used to calculate the SCST availability. Similar procedures can be applied for the SCMT, MCST, and MCMT scenarios to evaluate corresponding availability levels. Note, however, that the coverage area is not circular anymore when another criterion is adopted, as presented in the next subsection

D. SINR-based Availability Calculation

In order to analyze the SINR-based cell or system availability in the space domain as defined in Sec. VI, we need to calculate the area covered by the BS within the SINR threshold contour. Algorithm 1 illustrates the algorithm which is employed to create the SINR-based coverage contour. To further obtain space domain availability, the area of each Voronoi cell, which is decided by (19), will be used.

Refer to Cell number 6 in Fig. 5 as the reference cell. Fig. 7 illustrates the coverage contours of the BS in the reference cell with two different SINR thresholds, $Th = 0.4$ and 0.6 respectively where $\alpha = 2.5$. Therein, the coverage is no longer circular when using SINR as the criterion. Here we assume that the UEs are distributed uniformly across the whole network of interest.

A lower SINR threshold indicates that a UE can decode the received signal from the BS even though the signal strength is comparatively low. Thus it may still be connected

Algorithm 1: Algorithm to obtain the SINR threshold contour which represents the covered area of the BS.

Input: x_B, y_B : Cartesian coordinates of the BS of the RC
Input: N : Number of cells in the topology
Input: Th : SINR threshold
Input: α : Path loss coefficient
Output: x_p, y_p : Set of Cartesian coordinates along the SINR threshold contour

for $z = \frac{\pi}{180} : \frac{\pi}{180} : 2\pi$ *: z denotes the angle measured in radians.* **do**
  $d = 0.001$: d is the initial distance from the BS of the RC to any user
  $x_p(z) = x_B + d\ cos(z)$
  $y_p(z) = y_B + d\ sin(z)$
  $I(z) = 0$: $I(z)$ is the interference at the point $(x_p(z), y_p(z))$
  for $i = 1 : N$ **do**
    $dist(z,i) = \sqrt{(x_p(z) - x_B(i))^2 + (y_p(z) - y_B(i))^2}$: $dist(z,i)$ is the distance to the point $(x_p(z), y_p(z))$ from the i^{th} BS
    $I(z) = I(z) + dist(z,i)^{-\alpha}$
  end
  $SINR(z) = \frac{d^{-\alpha}}{I(z) - d^{-\alpha}}$
  while $SINR(z) \geq Th$ **do**
    $d = d + 0.001$
    $x_p(z) = x_B + d\ cos(z)$
    $y_p(z) = y_B + d\ sin(z)$
    $I(z) = 0$
    for $i = 1 : N$ **do**
      $dist(z,i) = \sqrt{(x_p(z) - x_B(i))^2 + (y_p(z) - y_B(i))^2}$
      $I(z) = I(z) + dist(z,i)^{-\alpha}$
    end
    $SINR(z) = \frac{d^{-\alpha}}{I(z) - d^{-\alpha}}$
  end
end

despite a longer distance to the tagged BS, which is the BS deployed in the same cell. Meanwhile moving away from the tagged BS within the cell means that the received power from the neighboring BSs becomes more significant. Consequently, the interference level in SINR calculations is higher. By thoroughly examining Fig. 7(a), we observe that the coverage contour is biased towards the reference cell where the neighboring BSs (in Cells 2, 3, and 4, Topology 1) are located in the proximity, and that the contour folds outwards where the neighboring BSs (in Cells 5, 7, and 10, Topology 1) are located farther away.

When a high SINR threshold is configured, a UE should locate within the range where the received power from the tagged BS is dominant versus the interference from other neighboring BSs in order to be covered. Since the effects from neighbor BSs are not significant due to distance in this case, the contour becomes much smoother and the shape of the coverage contour converges towards an approximate circular area, as shown in Fig. 7(b).

E. User-oriented Availability Calculation

For an end-user, it is essential to know whether the service is available or not at the location of the UE, represented by the *individual user-oriented availability* defined in Sec. VII. From a service provider's point of view, it is also important to know its offered services are available to how much percent of the users distributed within the network. This is measured by the *user-oriented system availability* defined herein.

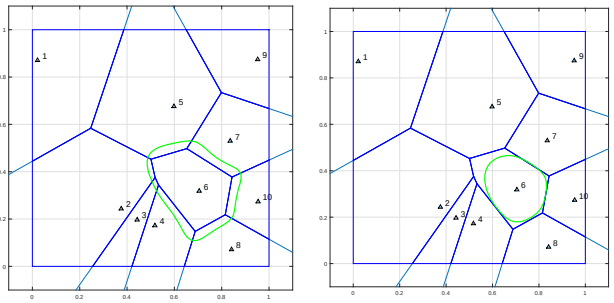

(a) SINR threshold $Th = 0.4$ (b) SINR threshold $Th = 0.6$

Fig. 7: The coverage contours with low and high SINR thresholds for Cell 6: A network view.

For the calculation of user-oriented system availability, the PV diagram has to be generated as the first step and then end users are distributed across those PV cells according to a homogeneous PPP distribution with intensity λ_U. As the next step, Algorithm 1 is used to create SINR threshold contours. Lastly we evaluate the user-oriented system availability as given in (18) by counting the number of UEs covered by the BSs collectively.

IX. Numerical Results from Availability Analysis

Based on the definitions and analysis presented in the previous sections, we present in this section the obtained numerical results with various network topologies and BS or UE distributions. The region of interest is configured as a unit area of 1×1. Unless otherwise stated, the parameters are configured as $\alpha = 2.5, 0.4 \leq Th \leq 0.6, N = 10$, and $M = 5$.

A. Connectivity-based Analysis: Cell Availability

Consider Fig. 1 as the SCST scenario and keep Cell 6 as the reference cell. For the SCMT scenario, the four topologies shown in Fig. 3 are used together with Fig. 1 to form $M = 5$ topologies. Fig. 8 illustrates the individual cell unavailability of the reference cell. The colored (dashed) curves are obtained based on (4) and they represent the obtained cell unavailability for Cell 6 under five topologies. For the SCMT scenario, the blue (solid with triangle marks) line is the average cell unavailability obtained based on $A_s^c(i,:)$, as expressed in (6).

As shown in the figure, the smaller the BS coverage, the higher the unavailability. As mentioned earlier, for connectivity-based availability analysis, we adopt simply πR^2 minus the exurban areas as the covered area of a BS where R is the BS transmission range. Accordingly, we observe that unavailability decreases monotonically to a substantially low level, as the BS transmission range becomes sufficiently high. With a large enough coverage, the achieved cell unavailability can be reduced to zero, implying that all users residing in the reference cell are connected to the network through the serving BS. For connectivity-based availability, attaining cell unavailability close to zero implies that URC in terms of space domain availability can be achieved within the cell.

Moreover, the discrepancy among these cell availability curves related to each topology is caused by the randomness of each deployment. As a consequence, higher unavailability

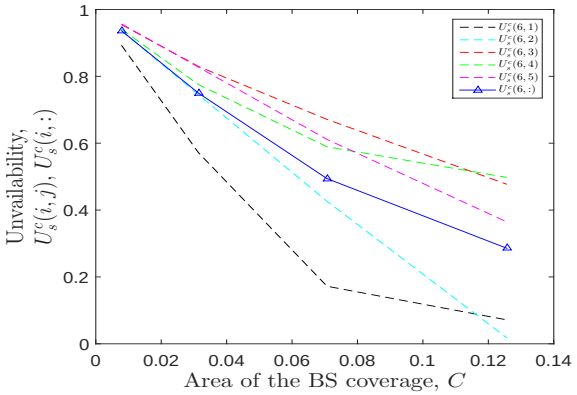

Fig. 8: SCST and SCMT cell unavailability of the reference cell, i.e., $i = 6$, for $M = 5$ topologies as the BS coverage increases.

is entailed where the reference cell occupies a larger cell area in the respective topology, and vice versa. This result implies that it may not be beneficial to deploy the same type of cells in a PV network. In other words, *the deployment of hybrid small-cells and macro-cells is recommended* [5].

To obtain cell availability in the MCST and MCMT scenarios, all N cells in the network need to be considered. Fig. 9 depicts the variation of unavailability for all 10 cells (in green dashed lines) based on Topology 1, as the BS coverage of the BS increases. The average cell unavailability of these 10 cells (in blue solid line with triangle marks) has been calculated using (6) for the MCST scenario based on the same topology.

B. Connectivity-based Analysis: System Availability

To obtain space domain system availability for a given network topology, as expressed in (9), we need to exclude the overlapping areas among neighboring cells. Based on Topology 1 shown in Fig. 1, we illustrate the obtained system unavailability in Fig. 9 (in red solid line with plus marks), as the BS coverage varies. For comparison purposes, we plot also in the same figure the individual cell unavailability for all 10 cells in the same network. When comparing the MCST cell unavailability (in blue) with the system unavailability (in red), we notice that the latter one has higher values for all BS coverage ranges. This is because to obtain system unavailability for any topology, the overlapping areas need to be excluded for coverage calculation.

When the coverages of the BSs are at their minimum values, the system unavailability reaches the peak, since the probability that a user could fall inside the uncovered area becomes highest. Increasing the radius of the BS coverage will obviously reduce the system unavailability of the cellular network. However as shown in Fig. 9, the individual cell availability varies dramatically from each other and some cells reach zero unavailability before the system unavailability does. This is caused by the diversity of cell sizes in a PV network. While cells which spread over a wider geographical area need relatively high transmission power to reduce unavailability of the cell, smaller cells reach this goal with comparably low transmission power. This implies that, to achieve URC, it may not be beneficial to uplift the transmission power for the whole network identically for all cells. In other words, deploying a

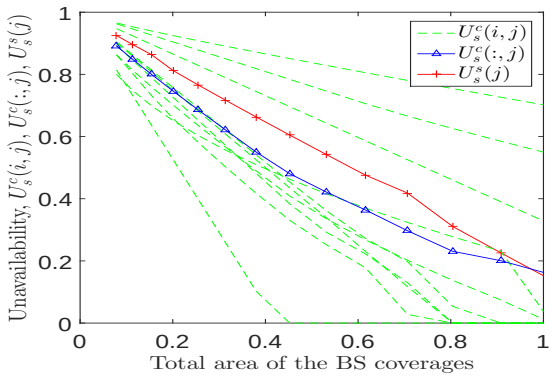

Fig. 9: SCST, MCST cell unavailability with 10 cells for topology $j = 1$, together with the system unavailability (in red) for this topology.

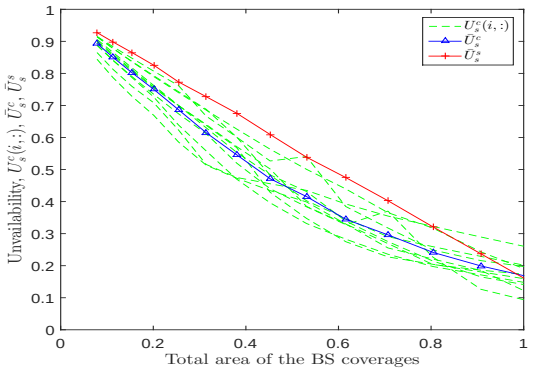

Fig. 10: SCMT, MCMT cell unavailability with 10 cells for 5 topologies, together with the average system unavailability.

hybrid network with different cell sizes would be advantageous from an operator's perspective.

Consider now multiple topologies to further analyze system unavailability in the space domain. Fig. 10 illustrates the system unavailability behavior (red solid line with plus marks) averaged over $M = 5$ topologies. To compare the results with the ones shown in Fig. 9, the SCMT cell unavailability (green dashed) and MCMT cell unavailability (blue solid line with triangle marks) are also included. Clearly, both cell unavailability and system unavailability exhibit a similar trend as shown in Fig. 9 when the coverage of the BSs increases. However, the curves become smoother since they are the average values obtained across multiple topologies.

C. SINR-based Availability Analysis

1) The effect of SINR threshold: For SINR-based availability analysis, let us first consider the SCST scenario in Topology 1 with the same reference cell. Fig. 12 illustrates the obtained $U_s^c(i,j)$ variation for Cell 6 as the SINR threshold increases. It can be observed that the achieved unavailability increases with a higher SINR threshold.

According to (14), when the SINR threshold is higher, the coverage boundary or contour is tighter, resulting in a smaller area of the BS coverage. On the other hand, unavailability is close to or reaches zero if the SINR threshold is sufficiently low, meaning that the BS can assure availability within the cell almost anywhere. With a higher SINR threshold, URC

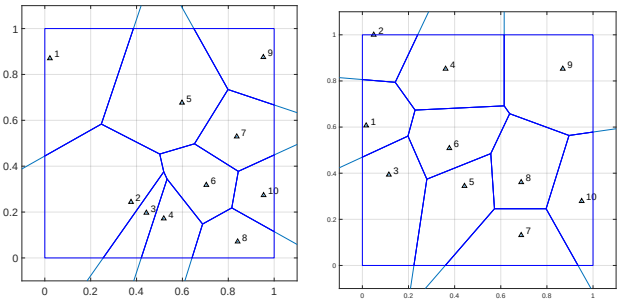

(a) PPP distributed BSs. (b) DPP distributed BSs.

Fig. 11: Homogeneous cellular network consisting of N = 10 cells.

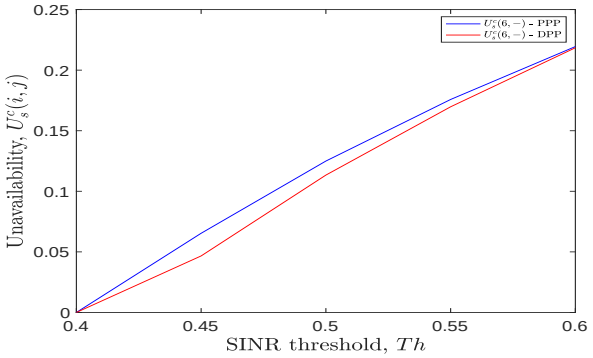

Fig. 12: SCST cell unavailability of the reference cell $(i = 6)$ as the SINR threshold varies: PPP versus DPP.

can be achieved if the BS has high enough transmission power and/or the neighboring BSs are located far enough away from the UE's location.

Furthermore, we have also investigated the availability performance of the same network by considering that BSs are distributed according to a DPP with the same intensity. The SCST availability results for the same reference cell, which are obtained based on the network topologies shown in Fig. 11, are illustrated in Fig. 12. As shown in the figure, the availability curves from both distributions exhibit the same trend as the SINR threshold increases. However, the availability level achieved in the DPP model is generally higher than that in the PPP model. This is because spatial correlation among BSs is considered in DPP and the BS locations are more evenly distributed in DPP when compared with in PPP. As a consequence, the reference cell in DPP experiences less interference than in PPP, leading to a higher received SINR level in the DPP case. However, when the SINR threshold is very low or very high, the availability difference between these two curves is negligible since the SINR contour areas have become too large or too small.

2) The effect of reference cell location: Extend the SCST scenario to the SCMT scenario as presented in Fig. 1 and Fig. 3. Fig. 13 illustrates the SCST cell unavailability of the reference cell under each topology (in dashed plots), together with the SCMT cell unavailability averaged over 5 topologies (in blue solid line with triangle marks). When $Th < 0.5$, $U_s^c(6,2)$ and $U_s^c(6,3)$ remain as zero, $U_s^c(6,5)$ attains zero, while $U_s^c(6,1)$ and $U_s^c(6,4)$ are positive. Furthermore, $U_s^c(6,5) < U_s^c(6,1) < U_s^c(6,4)$. This behavior is dependent on the location of the reference cell in each network

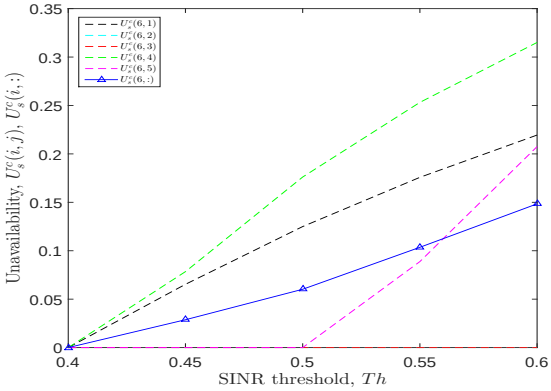

Fig. 13: SCST and SCMT cell unavailability for $i = 6$ and $M = 5$ topologies as the SINR threshold increases.

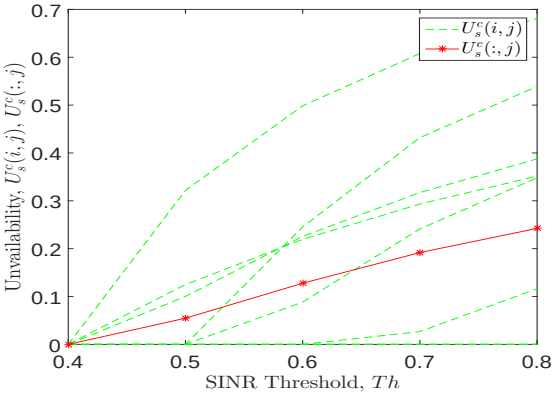

Fig. 14: SCST and MCST cell unavailability for $N = 10$ cells of topology $j = 1$ as the SINR threshold increases.

topology as well as its neighborhood, as explained below.

Among these 5 topologies, the reference cell is placed in the middle of the network only in Topology 1. In this case, it has 7 neighboring cells which generate interference to UEs in Cell 6. In all other 4 topologies shown in Fig. 3, the reference cell is placed closer to an edge of the unit square network, however, with different cell sizes and distances to the neighboring BSs. For instance, in Topology 2, the reference cell has only 3 neighboring cells located comparatively far away from it. Therefore, the interference level in Topology 2 is much lower than in Topology 1, leading to higher availability offered by the reference cell.

3) SINR-based availability for multi-cell and multi-topologies: Considering now all $N = 10$ cells in the network, Fig. 14 depicts the variation of cell unavailability as the SINR threshold varies under the SCST and MCST scenarios (in green dashed curves and red solid curve respectively). It can be observed that many cells located at the corners of the region achieve zero unavailability within the configured SINR threshold range due to less interference from neighboring cells. In general, however, the MCST cell unavailability shows a monotonically increasing behavior when the SINR threshold increases.

The SINR-based cell availability for the MCMT scenario is illustrated in Fig. 15 (in curves with black dashed plots) showing the MCST cell unavailability for each individual topology. The blue solid curve with triangle marks represents the MCMT cell unavailability averaged over all topologies.

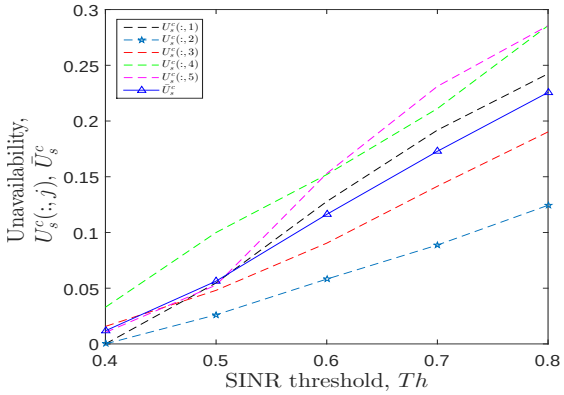

Fig. 15: MCMT cell unavailability for $N = 10$ cells and $M = 5$ topologies as the SINR threshold increases.

From this figure, a similar trend illustrating increased cell unavailability with a higher SINR threshold can be observed. However, the variation of this unavailability becomes more bounded when multiple topologies are considered. This result indicates that to obtain more stable behavior more topologies should be included.

D. Individual User-oriented Availability in a PV Network with PPP Distributed End-users

To obtain the individual user-oriented availability defined in Sec. VII, we need to identify whether a randomly selected end-user is located within the coverage of the BS in the same Voronoi cell or not. Since the coverage of a BS is dependent on the SINR threshold, we identify three cases representing the locations of a randomly selected UE. The UE is randomly picked up from a homogeneous PPP distribution with intensity $\lambda_U = 1500$ or $\lambda_U = 500$ in a 1×1 area, with three possible positions as shown in Fig. 16(a).

- Position 1 (P_1): A UE lies close to the BS within the contour of the covered area;
- Position 2 (P_2): A UE lies on or close to an edge of the cell, outside the coverage of the BS of the cell to which it belongs;
- Position 3 (P_3): A UE lies in-between the ranges of the areas covered by the SINR threshold contours configured with $0.5 \leq Th \leq 0.7$.

When a UE is placed close enough to a BS, i.e., within the smallest coverage contour, its individual user availability is 1, as obtained in Fig. 16(b). When a UE is located far away from the BS, i.e., outside the largest coverage contour according to the configured SINR threshold values, this availability is 0. When a UE is located at Position 3, whether it achieves its individual user-oriented availability as 1 or 0 depends on various conditions like the SINR threshold and the shape of the cells. For example, when a tight SINR threshold is given to all BSs and the BS coverage is close to the cell edge, a UE located comparatively far away from the BS can still be covered, obtaining its unavailability as 0. The blue solid line with triangle marks in Fig. 16(b) depicts the variation of the individual unavailability accordingly when the randomly selected UE falls between the coverage areas obtained from the configured SINR threshold range for Topology 1. At the SINR threshold value of $Th = 0.61$, the individual cell unavailability flips from 0 to 1.

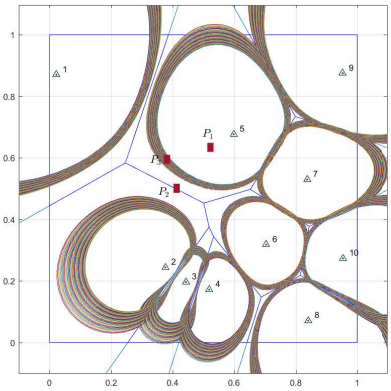

(a) Three possible positions of an individual user, i.e., P_1: UE lies inside the cell; P_2: UE lies on close to an edge of a cell; and P_3: UE lies in between the SINR contours.

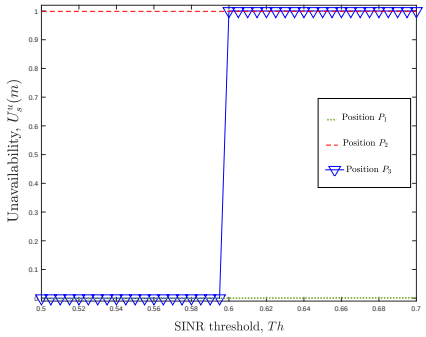

(b) The variation of individual user unavailability.

Fig. 16: Individual user unavailability for a randomly selected UE. The UE's three positions are marked as P_1, P_2 and P_3 respectively.

E. User-oriented System Availability of a PV Network with PPP Distributed End-users

Moreover, we investigate the user-oriented system availability in a PV network including UEs PPP distributed according to $\lambda_U = 1500$ in an area of 1×1. In addition to using SINR as the criterion for coverage calculations, we consider also the resource requirement for a user in terms of the obtained capacity in an OFDM system.

1) User-oriented system availability with SINR-based coverage contour: Configure the network under Topology 1 with a given intensity level for UE distributions and an identical SINR threshold for all 10 cells in the range of $0.4 \leq Th \leq 0.6$. We obtain first the coverage contour for each cell and then examine the individual user-oriented availability for all UEs in the whole network. As expressed in (18), the ratio between the number of covered UEs by all BSs and the total number of UEs in the network decides the system availability.

Fig. 17(a) and Fig. 17(b) illustrate respectively the coverage contours for this network and the obtained user-oriented system unavailability as the SINR threshold varies, with two user density levels $\lambda_U = 1500$ and 500 respectively. Fig. 17(b) illustrates that both curves increase monotonically with an increasing SINR threshold. This is because with a higher SINR threshold the coverage area of the BS shrinks, leading to a lower number of covered users by the BS. Meanwhile, although the total number of users is greatly increased when $\lambda_U = 1500$, a majority of them will be distributed in the

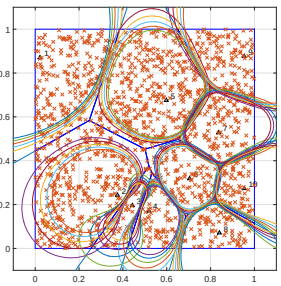

(a) The PV network with $\lambda_U = 1500$ PPP distributed end-users and SINR-based coverage contours.

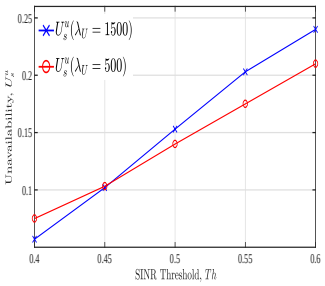

(b) The behavior of the user-oriented system unavailability as the SINR threshold varies with two difference UE intensities.

Fig. 17: The obtained user-oriented system unavailability as the SINR threshold varies for a PV network with PPP end-user distributions.

uncovered areas, i.e., the coverage holes, when the SINR threshold is high. Therefore, lower availability is observed for a large value of λ_U. On the other hand, when the users have a lower SINR requirement, the area covered by the SINR contours is larger. Then a larger λ_U value increases the number of users *inside* the coverage areas, leading to higher availability (or lower unavailability). For this reason, when $Th = 0.45$ or lower, the resulted unavailability with $\lambda_U = 1500$ is lower or much lower than that with $\lambda_U = 500$.

2) User-oriented system availability with capacity-based coverage contours: Homogeneous resource requirements: Consider in this case that a user is associated with a BS only when the achieved capacity meets the service requirement. For an OFDM cell, the instantaneous data rate, R_b, corresponds to the amount of bits in an OFDM symbol that can be transmitted through the channel within a duration of an OFDM symbol, expressed as [28]

$$R_b = \frac{nW(N_{used} - 1)log_2 M_{mod}}{N_{FFT}(1 + G)} R_{err}\beta, \qquad (20)$$

where W is the total bandwidth, N_{FFT} is the total number of sub-carriers, N_{used} is the number of used sub-carriers, M_{mod} is the number of data symbols in the constellation, G is the ratio between the guard time for an OFDM symbol and the used OFDM symbol time, n is the oversampling factor, R_{err} is the error-correcting code rate, and β is the ratio between the number of data sub-carriers and the number of pilot sub-carriers and data sub-carriers.

When considering a homogeneous resource requirement, we consider that all end-users in the network have an identical resource requirement, i.e., the same capacity as obtained by (20). Fig. 18(a) illustrates the obtained capacity threshold boundaries together with $\lambda_U = 500$ PPP distributed end-users dispersed within a PV network. Accordingly, the user-oriented system unavailability for such a network can be obtained, as shown Fig. 18(b). As observed from this figure, the obtained user-oriented system unavailability increases monotonically when users have a higher capacity requirement. Similar to the SINR-based analysis, a BS can only serve a smaller area when the capacity requirement becomes higher. Accordingly, the number of served end-users is reduced, leading to higher unavailability.

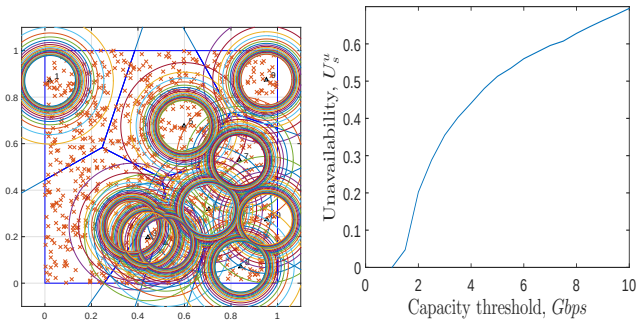

(a) The PV network with $\lambda_U = 500$ PPP distributed users and capacity-based threshold contours.

(b) The behavior of the user-oriented system unavailability as the capacity threshold varies.

Fig. 18: The obtained user-oriented system unavailability for end-users with a homogeneous capacity requirement.

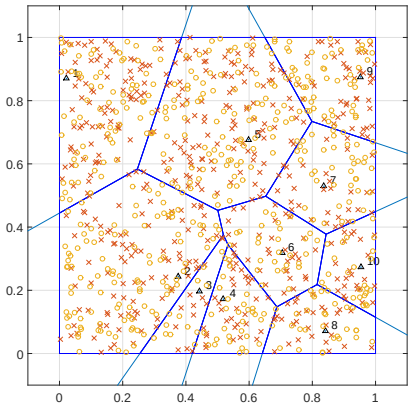

Fig. 19: A PV network consisting of 10 BSs and end-users with $\lambda_U = 500$ following two independent PPP distributions. The empty circles and cross symbols represent LRR and HRR end-users respectively.

3) User-oriented system availability with capacity-based coverage contours: Heterogeneous resource requirements: In real-life scenarios, end-users have different bandwidth or capacity requirements, referred to as heterogeneous resource requirements in this study. For the numerical results presented in this subsection, we consider two types of users, i.e., low resource requiring (LRR) users requiring N_{used} number of OFDM sub-carriers and high resource requiring (HRR) users requiring $2 \times N_{used}$ sub-carriers. Their spatial distributions are illustrated in Fig. 19.

Fig. 20 illustrates the obtained user-oriented system unavailability under the heterogeneous requirement scenario for LRR and HRR users respectively. It is worth mentioning that the total capacity shown as the x-axis in Fig. 20 is the total capacity of a cell and it is offered to both LRR and HRR users together in the cell. The cell capacity for each cell in this network is assumed to be identical. In general, the user-oriented system unavailability decreases when the network offers higher capacity. Since HRR end-users require a higher data rate in order to get served, their unavailability curve keeps at a higher level in comparison with that of LRR end-users.

The reason for these results is as follows. For a cell with a fixed number of sub-carriers, the number of end-users which can be served by the network would reduce when users have a higher resource requirement. Furthermore, since an HRR user requires a higher data rate than an LRR user does, a smaller number of HRR users can be served for any given total capacity. Thus the system unavailability of the network for HRR users is higher than that for LRR users.

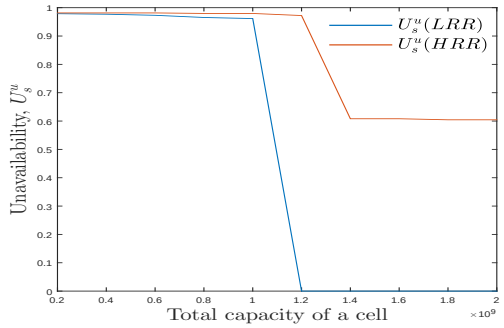

Fig. 20: User-oriented system unavailability variation for LRR and HRR users when the capacity threshold increases.

X. An Algorithm for Availability Improvement

Finally, we propose an algorithm that can be adopted by operators for the purpose of availability enhancement based on the calculated availability level. When the observed cell availability level is lower than a certain threshold, an operator can take various actions to improve availability, e.g., by deploying more small cells, traffic offloading, or load balancing. In this section, we present this algorithm by introducing a relay node at the edge of the reference cell.

Considering the same network topology as shown in Fig. 1, we introduce a relay node which is located as the edge of Cell 6, as shown in Fig. 21(a). Assume that a fiber-optic backhaul link exists between the macro BS and the relay node. The relay node is already deployed but it is activated in an on-demand manner and its transmit power level is adjustable.

A step-by-step procedure of this algorithm is shown in Algorithm 2 and it is targeted at any cell of interest. To calculate the cell availability of cell i at topology j *after relay assisted enhancement*, (4) needs to be updated as follows,

$$A_s^c(i,j) = \frac{C(i,j) + RL(i,j) - \Delta'}{S(i,j)} \tag{21}$$

given that $C(i,j) + RL(i,j) - \Delta' \leq S(i,j)$. In (21), $RL(i,j)$ and Δ' denote the covered area of the relay node of cell i at topology j and overlapped area between the macro BS (cell i at topology j) and the relay node respectively.

Algorithm 2: Algorithm to activate the relay node.

Input: $A_1, A_2, \cdots, A_n$ Cell availability threshold values where $A_1 < A_2 < \cdots < A_n$
Input: $PW_1, PW_2, \cdots, PW_n$ Relay node transmit (Tx.) power levels where $PW_1 > PW_2 > \cdots > PW_n$
Output: PW_n Transmit power of the relay node
Calculate cell availability $A_s^c(i,j)$ based on (4)
if $A_s^c(i,j) \leq A_1$ **then**
  Activate the relay node with Tx. power $= PW_1$
else if $A_1 < A_s^c(i,j) \leq A_2$ **then**
  Activate the relay node with Tx. power $= PW_2$
$\cdots$
else if $A_{n-1} < A_s^c(i,j) < A_n$ **then**
  Activate the relay node with Tx. power $= PW_n$
else
  Do not activate the relay node. */ This condition indicates that the designed availability level (i.e., $A_s^c(i,j) \geq A_n$) is achieved. /*
end

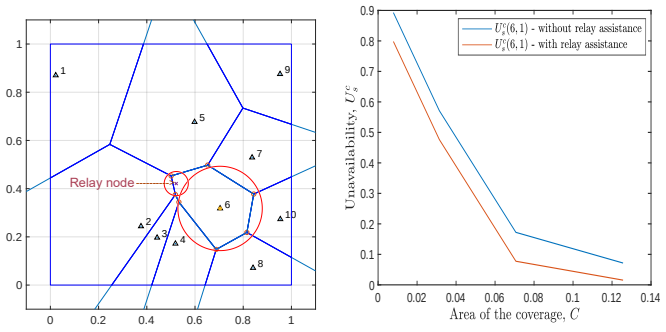

(a) The PPP distributed homogeneous cellular network including a relay node in cell number 6.

(b) The obtained SCST cell unavailability of the reference cell: With versus without the relay node.

Fig. 21: Cell availability improvement by deploying a relay node.

As observed in Fig. 21(b), the deployed relay node has contributed positively to achieve higher availability of the reference cell compared with the macro BS only case. Moreover, the proposed algorithm is able to decide when to activate the relay node as well as its transmit power level based on the measured availability metric. Herein, we do not suggest any concrete values as the availability thresholds A_i and transmit power levels PW_i where $i = 1, 2, \cdots, n$. When employing such an algorithm in real-life networks, the PW_i values need to be configured such that the relay node can reduce the coverage holes as much as possible to meet the designed availability level A_n while considering the operational and power consumption cost.

XI. Conclusions and Future Work

In this paper, we performed a dependability theory based availability analysis addressing how to achieve ultra-reliable communication in the space domain in 5G networks. The space domain availability definitions advocated in this paper address the *anywhere* aspect of anytime and anywhere service provisioning. To perform space domain availability analysis, one may adopt a connectivity-based, SINR-based, or capacity-based criterion for coverage calculations. Furthermore, the user-oriented availability analysis affords an insight for an operator on the availability level it provides, as well as the tradeoff between cell capacity/BS transmission power, or user resource requirements, and cell or system availability. In order to achieve a satisfactory level of space domain availability, a fine-tuned orchestration among various factors or parameters, like heterogeneous BS deployments including both macro- and small-cells, BS transmission power, SINR threshold, resource requirements for end-users, is recommended. As our future work, we plan to investigate other techniques for availability enhancement such as load balancing and device-to-device communication based on real-life availability measurements, especially for newly launched services like LTE-M and narrowband Internet of things (NB-IoT).

References

[1] 3GPP TR 38.824, "Study on physical layer enhancements for NR ultra-reliable and low latency case (URLLC)," R16, v16.0.0, Mar. 2019.

[2] METIS-II, Deliverable D5.2, "Final considerations on synchronous control functions and agile resource management framework for 5G," Mar. 2017, [Online]. Available: https://metis-ii.5g-ppp.eu/documents/deliverables/.

[3] ITU-T, "Terms and definitions related to quality of service and network performance including dependability," Recommendation E. 800, 1994.

[4] A. Avižienis, J.-C. Laprie, B. Randell, and C. Landwehr, "Basic concepts and taxonomy of dependable and secure computing," *IEEE Trans. Depend. Sec. Comput.*, vol. 1, no. 1. pp. 11-33, Mar. 2004.

[5] H. V. K. Mendis and F. Y. Li, "Achieving ultra reliable communication in 5G networks: A dependability perspective availability analysis in the space domain," *IEEE Commun. Lett.*, vol. 21, no. 9, pp. 2057-2060, Sep. 2017.

[6] P. Popovski, V. Braun, and H. Mayer, "Deliverable D1.1 scenarios requirements and KPIs for 5G mobile and wireless system," Apr. 2013, [Online]. Available: https://www.metis2020.com/wp-content/uploads/deliverables/METIS_D1.1_v1.pdf.

[7] P. Popovski, "Ultra-reliable communication in 5G wireless systems," in *Proc. 1st Int. Conf. 5G Ubiquitous Connectivity*, Nov. 2014, pp. 146-151.

[8] R. Vaze, "Throughput-delay-reliability tradeoff with ARQ in wireless ad hoc networks," *IEEE Trans. Wireless Commun.*, vol. 10, no. 7, pp. 2142-2149, Jul. 2011.

[9] H. Beyranvand, M. Lévesque, M. Maier, J. A. Salehi, C. Verikoukis, and D. Tipper, "Toward 5G: FiWi enhanced LTE-A HetNets with reliable low-latency fiber backhaul sharing and WiFi offloading," *IEEE/ACM Trans. Netw.*, vol. 25, no. 2, pp. 690-707, Apr. 2017.

[10] M. Goyal, S. Prakash, W. Xie, Y. Bashir, H. Hosseini, and A. Durresi, "Evaluating the impact of signal to noise ratio on IEEE 802.15.4 PHY-level packet loss rate," in *Proc. IEEE Network-Based Information Systems (NBiS)*, Sep. 2010, pp. 279-284.

[11] X. Ma, X. Yin, G. Butron, C. Penney, and K. S. Trivedi, "Packet delivery ratio in k-dimensional broadcast ad hoc networks," *IEEE Commun. Lett.*, vol. 17, no. 12, pp. 2252-2255, Dec. 2013.

[12] I. A. M. Balapuwaduge, F. Y. Li, and V. Pla, "System times and channel availability for secondary transmissions in CRNs: A dependability-theory-based analysis," *IEEE Trans. Veh. Technol.*, vol. 66, no. 3, pp. 2771-2788, Mar. 2017.

[13] H. D. Schotten, R. Sattiraju, D. G. Serrano, Z. Ren, and P. Fertl, "Availability indication as key enabler for ultra-reliable communication in 5G," in *Proc. IEEE European Conference on Networks and Communications (EuCNC)*, Jun. 2014, pp. 1-5.

[14] I. A. M. Balapuwaduge and F. Y. Li, "A joint time-space domain analysis for ultra-reliable communication in 5G networks," in *Proc. IEEE ICC*, May 2018, pp. 1-6.

[15] F. Baccelli, M. Klein, M. Lebourges, and S. Zuyev, "Stochastic geometry and architecture of communication networks," *Telecommunication Systems*, vol. 7, no. 1, pp. 209-227, Jun. 1997.

[16] F. Baccelli and S. Zuyev, "Stochastic geometry models of mobile communication networks," *Frontiers in Queueing: Models and Applications in Science and Engineering*, 1996, pp. 227-243.

[17] T. X. Brown, "Cellular performance bounds via shotgun cellular systems," *IEEE J. Sel. Areas Commun.*, vol. 18, no. 11, pp. 2443-2455, Nov. 2000.

[18] S. Lee and K. Huang, "Coverage and economy of cellular networks with many base stations," *IEEE Commun. Lett.*, vol. 16, no. 7, pp. 1038-1040, Jul. 2012.

[19] J. G. Andrews, F. Baccelli, and R. K. Ganti, "A tractable approach to coverage and rate in cellular networks," *IEEE Trans. Commun.*, vol. 59, no. 11, pp. 3122-3134, Nov. 2011.

[20] F. Muhammad, Z. Abbas, and F. Y. Li, "Cell association with load balancing in nonuniform heterogeneous cellular networks: Coverage probability and rate analysis," *IEEE Trans. Veh. Technol.*, vol. 66, no. 6, pp. 5241-5255, Jun. 2017.

[21] Y. Li, F. Baccelli, H. S. Dhillon, and J. G. Andrews, "Statistical modeling and probabilistic analysis of cellular networks with determinantal point processes," *IEEE Trans. Commun.*, vol. 63, no. 9, pp. 3405-3422, Jul. 2015.

[22] 3GPP TS 37.320, "Universal terrestrial radio access (UTRA) and evolved universal terrestrial radio access (E-UTRA); radio measurement collection for minimization of drive tests (MDT); overall description; stage 2," R13, v13.1.0, Apr. 2016.

[23] T. Bai and R. W. Heath, "Location-specific coverage in heterogeneous networks," *IEEE Sig. Proces. Lett.*, vol. 20, no. 9, pp. 873-876, Sep. 2013.

[24] S. Mukherjee, "Distribution of downlink SINR in heterogeneous cellular networks," *IEEE J. Sel. Areas Commun.*, vol. 30, no. 3, pp. 575-585, Apr. 2012.

[25] P. Madhusudhanan, J. G. Restrepo, Y. Liu, T. X. Brown, and K. R. Baker, "Downlink performance analysis for a generalized shotgun cellular system," *IEEE Trans. Wireless Commun.*, vol. 13, no. 12, pp. 6684-6696, Dec. 2014.

[26] L. Chiaraviglio, F. Cuomo, M. Maisto, A. Gigli, J. Lorincz, Y. Zhou, Z. Zhao, C. Qi, and H. Zhang, "What is the best spatial distribution to model base station density? A deep dive in two European mobile networks," *IEEE Access*, vol. 4, pp. 1434-1443, May 2016.
[27] H. Pham, *System Software Reliability*. London, UK: Springer, 2007, Ch.2 System Reliability Concepts, pp. 9-75.
[28] S. C. Yang, *OFDMA System Analysis and Design*. Norwood, MA, USA: Artech House, 2010.
[29] M. de Berg, O. Cheong, M. van Kreveld, and M. Overmars, *Computational Geometry Algorithms and Applications*. 3rd Ed. Berlin, Germany: Springer-Verlag, 2000.
[30] R. Pure and S. Durrani, "Computing exact closed-form distance distributions in arbitrarily-shaped polygons with arbitrary reference point," *The Mathematica Journal*, vol. 17, pp. 1-27, Jun. 2015.

Kalpanie Mendis received the B.Sc. Engineering (Honors) degree in Electrical and Information Engineering from University of Ruhuna, Sri Lanka, in 2015, and pursued her Masters Degree in Information and Communication Technology (ICT) at the University of Agder (UiA), Norway. Her Master thesis with the focus on 5G Ultra-reliable communications was awarded as the Best Master's thesis in ICT at UiA in 2017. Currently she is a doctoral research fellow at the Department of Information Security and Communication Technology at the Norwegian University of Science and Technology (NTNU), Norway. She has worked as a lecturer at the Department of Electrical and Information Engineering, University of Ruhuna from May 2014 to July. 2015. Her current research interests lie on the areas of 5G ultra reliable and low latency communications, end-to-end network slicing, multi-RAT architectures, software defined networking, network function virtualization, and management and orchestration of networks.

Indika A. M. Balapuwaduge (S'12-M'17) received the B.Sc. Engineering (First Class Honors) degree from University of Ruhuna, Sri Lanka, in 2008, and the M.Sc. and the Ph.D. degrees in Information and Communication Technology (ICT) from University of Agder (UiA), Norway in 2012 and 2016, respectively. His Master thesis was awarded as the Best Master's thesis in ICT at UiA in 2012. Currently he is a Post-Doctoral Research Fellow at the Department of ICT, UiA. He spent one year as an engineer at Huawei technologies, Sri Lanka, from Oct. 2008 to Aug. 2009 and he worked as a lecturer at the Department of Electrical and Information Engineering, University of Ruhuna from Aug. 2009 to Aug. 2010. Dr. Indika's current research interest covers various areas of mobile and wireless communications, including cognitive radio networks, ultra-reliable communication, massive MTC, Internet of Things, modeling and performance analysis of modern communications systems and networks.

Frank Y. Li (S'99-M'03-SM'09) received the Ph.D. degree from the Department of Telematics, Norwegian University of Science and Technology (NTNU), Trondheim, Norway. He worked as a Senior Researcher at UniK-University Graduate Center (now Department of Technology Systems), University of Oslo, Norway before joining the Department of Information and Communication Technology, University of Agder (UiA), Agder, Norway, in August 2007 as an Associate Professor and then a Full Professor. During the past few years, he has been an active participant in several Norwegian and EU research projects. He is listed as a Lead Scientist by the European Commission DG RTD Unit A.03-Evaluation and Monitoring of Programmes in Nov. 2007. Dr. Li's research interests include MAC mechanisms and routing protocols in 5G mobile systems and wireless networks, mesh and ad hoc networks; wireless sensor network; D2D communication; cooperative communication; cognitive radio networks; green wireless communications; Internet of Things; reliability in wireless networks, QoS, resource management and traffic engineering in wired and wireless IP-based networks; analysis, simulation and performance evaluation of communication protocols and networks.